Green Chemistry

PAPER

View Article Online
View Journal | View Issue

Cite this: *Green Chem.*, 2025, **27**, 9992

Biobased amide surfactants derived from cellulose-waste hydroxy acids: mechanochemical synthesis, foam fractionation and performance†

Giorgia Crigna, *[a] Davide Moscatelli [b] and Tuomo Sainio *[a]

A series of hydroxycarboxylic acids (HAs) with excellent hydrophilic properties are produced from alkali treatment of cellulose-containing materials. The great majority of these hydroxy acids are glucoisosaccharinic acids (GISAs), which are promising starting materials for surfactant synthesis. Amide surfactant mixtures were produced by combining these HAs with primary amines of various alkyl chain lengths, namely, 12, 16 and 18 carbons. The reactions were performed under liquid-assisted grinding (LAG) conditions, a type of mechanochemical synthesis employing small quantities of liquid, water in this case, to favour the homogenization. Yields up to 90% were achieved with the purchased GISAs and up to 85% in terms of GISA–amides using non-purified HA mixtures, regardless of the amine used. Products derived from other HAs were detected as well. The amount of water influenced the efficacy of the mechanical stimuli and, hence, the yield of the reactions. Foam fractionation was employed as an alternative purification method and was effective in enriching the surfactants up to 33% in the described setup. The resulting GISA–amides were able to lower the water surface tension below 27, 31, and 34 mN m^{-1} for the 12-, 16- and 18-carbon alkyl chains, respectively. The surfactants were also able to form foams and emulsions. Preliminary considerations using data-fitting software and comparison with commercial surfactants (*e.g.*, SPAN® 20, MEGA-12, and MEGA 14) showed excellent potential in terms of possible applications and biodegradability.

Received 11th April 2025,
Accepted 16th July 2025

DOI: 10.1039/d5gc01806d

rsc.li/greenchem

Green foundation

1. In this work, we used mechanochemical synthesis to produce biobased and biodegradable surfactants utilising waste cellulose materials. With this reaction method, we avoided the use of solvents, catalysts or heat, using only small quantities of water to enhance the homogeneity of the system, with reaction times of less than 15 minutes. In addition, a green purification method, foam fractionation, was successfully applied to purify the surfactant mixtures.
2. Rather than using glucose or other high value materials, we exploited, without any further purification, waste streams such as pulping black liquor or alkali-treated cellulose waste. The reactions reached yields of up to 85% in terms of the targeted molecules. Foam fractionation was able to enrich the purity up to 33% in a very simple setup.
3. Additional research is needed to improve the sustainability of the production of alkyl amines and also to design a more efficient setup for foam fractionation.

1. Introduction

Surfactants are broadly used in many industrial processes, consumer goods and domestic applications. Their widespread use results in very large production volumes, which are unavoidably connected to many environmental issues related to raw materials and end of life. As environmental regulations become more stringent, there is increasing interest in sustainable surfactants.[1] Conventional surfactants are mostly produced from non-renewable and/or non-sustainable sources, and even if bio-based surfactants are already common, they are often produced from first generation raw materials, which are responsible for phenomena like deforestation, pesticide pollution, soil erosion and loss of biodiversity. Surfactants are also among the most challenging emerging contaminants and are continuously discharged into the environment through wastewater treatment plants.[2]

To address these sustainability issues, waste feedstocks can be used as raw materials in production, resulting in lower emission, renewable, bio-based and biodegradable surfactants.

[a]*Lappeenranta–Lahti University of Technology, Department of Separation Science, Mukkulankatu 19, 15210 Lahti, Finland. E-mail: tuomo.sainio@lut.fi, giorgia.crigna@lut.fi*
[b]*Department of Chemistry, Materials and Chemical Engineering "Giulio Natta", Politecnico di Milano, Via Mancinelli 7, 20131 Milano, Italy*

† Electronic supplementary information (ESI) available. See DOI: https://doi.org/10.1039/d5gc01806d

Among bio-based materials, cellulose represents the most abundant biopolymer on Earth; it is the main constituent of plant cell walls, but it can also be found in algae, fungi, and bacteria. Consequently, cellulose-based waste is plentiful, and, even if biodegradable, it represents a significant source of carbon emissions. Hence, methods for repurposing this raw material are being researched.[3]

When treated under alkaline conditions and at high temperatures, cellulose undergoes degradation, resulting in a series of hydroxycarboxylic acids (HAs). The main fraction consists of volatile HAs such as formic and acetic acids, low molecular weight acids such as lactic, glycolic and 2-hydroxybutanoic (2-HBA) acids and high molecular weight acids such as 2,5-dihydroxypentanoic acid (2,5-DHPA) and α- and β-glucoisosaccharinic acids (GISAs). This degradation occurs, for example, in the Kraft and soda pulping processes, which produce the waste material called 'black liquor', an alkaline side stream which contains, along with lignin, the aforementioned HAs.[4–6] The valorisation of this feedstock has been long investigated as a possible source of HAs as an alternative to using them as fuel. While some of these HAs already have known uses, *e.g.*, acetic, glycolic, lactic, and formic acids, others are still being explored as possible bio-chemicals.[7] Waste streams containing cellulose have also been treated with alkali to produce these hydroxy acids, as in the cases of agricultural waste and cotton-based textile waste.[8–11]

Among these acids, the ones that are of particular interest are glucoisosaccharinic acids (GISAs). GISAs possess many hydroxy groups as well as the carboxylic acid functionality, making them very versatile in terms of reactions, as they can act both as alcohols and acids. In addition, they undergo internal esterification under acidic pH conditions, resulting in lactones. They have been mostly studied for their capability of complexing metals.[12–14] In addition, their structure resembles that of sugars; for this reason, they look appealing in the production of sustainable surfactants.[6,7,15] Carbohydrates and their derivatives (*e.g.*, sorbitan, glucose, sucrose, *etc.*) are already utilised in the production of bio-based surfactants.[16] Cellulose itself is already employed as hydrophilic group for surfactants thanks to its enhanced hydrophilicity. The most common sugar-based surfactants are in the form of esters, glycosides/ethers, or amides. These types of surfactants are usually employed in consumer products thanks to their excellent biocompatibility and biodegradability.[16–20] GISA-based surfactants are expected to have comparable characteristics to sugar-based surfactants due to their similar chemical structure and reactivity.

Presently, only two known studies have documented the use of GISAs in surfactant production. In one study, α-GISA was employed in the catalytic production of ester surfactants using tall oil as a hydrophobic chain. In the study, a 40% yield was achieved after 24 hours at 70 °C in a microwave reaction.[21] Another study reported the thermal synthesis of GISAs–amide surfactants. The reaction was performed at relatively high temperatures (120 °C–170 °C) for three hours without the use of a catalyst in chloroform as solvent using fatty alkyl amines.[22] Amide-based surfactants, in comparison to esters and ethers/glycosides, display better stability due to the nature of the amide bond, which is stronger and consequently more resistant to hydrolysis due to resonance stabilization.[23] Amides perform better in alkali and acid conditions, which are typical, for example, of cleaning formulations. Their molecular structure, characterised by enhanced hydrogen bonding, confers them great emulsifying and thickening capabilities and good solubility.[24,25] Therefore, the decision was made to produce surfactants with amide bonds employing alkyl amines.

Long-chain alkyl amines can also be produced from bio-based waste materials, such as exhaust oils or non-edible triglycerides. There are different methods to produce primary amines; the traditional approaches require high temperatures, pressurized hydrogen, and metal catalysts for different catalytic reactions and hydrogenation.[26–29] Recent research has shown that these catalytic steps can be replaced with enzymatic synthesis, making the production of amides much more sustainable. Citoler *et al.* achieved amine synthesis through a one-pot tandem cascade performed by a carboxylic acid reductase (CAR) and a transaminase (ω-TA). Saturated and unsaturated fatty acids with carbon chain lengths ranging from C6 to C18 were successfully aminated, obtaining conversions of up to 96%.[30] In another work, Citoler *et al.* repeated this process using renewable triglycerides and adding a lipase-catalysed step.[31]

The amidation reaction itself requires harsh conditions, such as high temperatures and extended reaction times. As an alternative to thermal amidation, compounds such as chlorides, coupling reagents, and boron-based or transition metal catalysts can be used for amidation. All these methods become less effective when the reactants are sterically hindered, like in the case of fatty amines.[32] To address the problem of intensive reaction conditions and solubility issues, one promising technique is mechanically enhanced synthesis (or mechanosynthesis). This approach employs mechanical stimuli to induce the reaction of solids, drastically reducing the volume of solvents needed. Mechanochemistry has proven to be very effective for a wide variety of compounds and materials, such as pharmaceuticals peptides and organometallic compounds.[33,34] The addition of a small amount of liquid can greatly enhance or even enable mechanochemical reactions by significantly improving the mixing process, resulting in greater homogeneity and enhancing the molecular diffusion. This type of mechanical synthesis is called liquid-assisted grinding (LAG). LAG is defined by the parameter $\lambda = mL_{LAG}\ g_{reactants}^{-1}$, which is the ratio between the liquid additive and the total weight of the reactants.[35,36]

In order to be defined as LAG, the value of λ should be greater than 0 but smaller than 1 mL g^{-1} or 2 mL g^{-1} (some sources disagree[34,35,37]). In the case of long alkyl groups, such as those involved in surfactant synthesis, mechanical stimuli are indeed able to unwrap the long chains, increasing the contact area between the reactants and overcoming steric and mass transfer limitations.[38]

A. Bil *et al.* presented the mechanosynthesis of amides at room temperature without catalysts and with limited use of solvents and short reaction times. The authors investigated the LAG aminolysis of glyconolactones using various types of amines and water as the liquid additive. The reaction resulted in a 90% yield in a ball-mill system and an 83% yield in a pestle–mortar system for γ-galactonolactone and dodecylamine.[37] Herrlé *et al.* reported the synthesis of levoglucosenone amides in LAG mechanochemical conditions using both primary and secondary amines, obtaining some compounds with surfactant properties. They also proceeded with the sulfonation to obtain ionic surfactants.[39]

Purification of surfactants can be complex, since they can form stable emulsions, suspend solids, and enhance the solubility of impurities. Conventional methods, such as solvent extraction, chromatographic fractionation, and distillation, can still be adopted for the purification of surfactants; however, another strategy would be to exploit surfactant's interfacial activity, resulting in a less intensive purification. Their peculiar behaviour that allows them to form structures like micelles and foams can be exploited for the purpose of separating them from the reaction mixtures. Since amides exhibit good foaming characteristics, foam fractionation seems particularly suitable. The foam collected at the top of the column in fact undergoes phenomena like drainage, leaving the so-called dry foam which is composed of a more concentrated surfactant solution.[40–42] Chen *et al.* performed foam fractionation on surfactin, a natural lipopeptide, and reached enrichments up to 50% in batch and 55% in continuous mode.[43,44] Li *et al.* used foam fractionation on saponins, enriching the surfactant solution by 133-fold.[45]

In this work, the HAs mixtures employed in the surfactant synthesis were produced from different cellulose-like sources and used without any further purification. This minimized the number of steps necessary for the production of surfactants, reducing their overall impact and simplifying the process. These were then reacted with purchased fatty amines (namely, dodecyl-, hexadecyl- and octadecyl-amine) to produce bio-based surfactants. The reactions were conducted under liquid-assisted grinding (LAG) conditions both in a pestle–mortar system and in a rotary ball mill to ensure reproducibility. Purification options, including silica gel chromatography, recrystallisation and foam fractionation, were explored for possible post processing. Finally, the surfactants were studied in terms of their solution behaviour and physicochemical characteristics to determine their suitability for domestic and industrial applications.

2. Materials and methods

2.1 Materials

Microcrystalline cellulose (ThermoFisher Scientific), sodium hydroxide (98%, ThermoFisher Scientific), and CS11GC strong acid cation exchange resin (SAC) (FINEX/Johnson Matthey) were used for the production of hydroxy acid mixtures. Waste sources included zero fiber sludge, *i.e.*, sedimented pulpmill waste (ZFS) (Lake Näsijärvi, Tampere) and lactose (ThermoFisher Scientific).

For surfactant synthesis, dodecyl amine (98%, ThermoFisher Scientific), hexadecyl amine (90%, Sigma-Aldrich), and octadecyl amine (80%, Sigma-Aldrich) were combined with the hydroxy acids and with calcium α-D-isosaccharinate (98%, ThermoFisher Scientific). Deionized water (DIW, Evoqua, 0.104 μS cm^{-1}) was used throughout all the procedures.

Commercially available hydroxy acids (HAs) were used for the identification and quantification of the HAs in the mixtures. These included formic acid (98%–100%, for analysis, Merck KGaA), acetic acid (99%–100%, glacial, chemically pure, VWR), glycolic acid (99%, Acros Chemicals), succinic acid (99.5%, AnalaR Normapur, VWR), lactic acid (90% aqueous solution, chemically pure, VWR), sodium salt of 2-hydroxybutyric acid (2-HBA 97%, Sigma-Aldrich, CAS 5094-24-6), 2,5-dihydroxypentanoic acid (2,5-DHPA, 99%, Sigma-Aldrich), and calcium α-D-isosaccharinate (98%, ThermoFisher Scientific).

For HPLC analysis, acetonitrile (VWR Chemicals, chromatography grade), formic acid (VWR Chemicals, chromatography grade), phosphoric acid (VWR Chemicals, chromatography grade), and sodium phosphate (VWR Chemicals, chromatography grade) were used in the eluent preparation.

The purification of reaction mixtures involved the use of n-hexane (ThermoFisher Scientific, chromatography grade), silica gel (Sigma-Aldrich, high purity grade, pore size 60 Å, 60–100 mesh), isopropanol (VWR Chemicals, chromatography grade), acetonitrile (VWR Chemicals, chromatography grade), methanol (VWR Chemicals, chromatography grade), and ethanol (VWR Chemicals, chromatography grade).

Octanol (Honeywell, ≥99%), sunflower seed oil (*Helianthus annus*, Sigma-Aldrich) and sorbitan laurate (SPAN® 20, Sigma-Aldrich, MW = 346.46 g mol^{-1}) were used in the surfactants' characterisation.

2.2 Synthesis of the hydroxy acids (HAs)

A total of 1 kg of microcrystalline cellulose (MCC) was mixed with 5.1 L of 15% NaOH solution at a solid–liquid volumetric ratio of 1 : 6. The reaction was conducted in an air bath reactor, an oven equipped with six autoclave chambers that rotate around a central shaft. Four of the six autoclaves, each with a 2 L capacity, were filled to 70% and purged with nitrogen gas three times to remove air. No additional pressure was applied. The digestion was performed at 160 °C for a total of 6 hours, including 1 hour for heating to the target temperature and 5 hours of reaction time. The resulting black liquor containing the HAs was treated with CS11GC strong acid cation exchange resin (SAC) to convert the HAs from their sodium salt form to their acidic form by lowering the pH to approximately 2. The HAs were then dried overnight at 80 °C–105 °C before use.

Similarly, zero fibre sludge (ZFS) was subjected to alkali digestion using a 10% w/w NaOH solution. The digestion was performed at 180 °C for 3 hours in the air bath reactor. The resulting mixture underwent the same SAC resin treatment to

liberate the HAs from their salts, and the HAs were subsequently dried overnight at 80 °C–105 °C.

For lactose, the alkali digestion was carried out using a 4% calcium hydroxide ($Ca(OH)_2$) solution (3.6 L of water and 162 g of $Ca(OH)_2$) with a solid–liquid volumetric ratio of 1 : 6. The alkali solution was mixed with 600 g of lactose. The reaction was conducted at 90 °C for 13 hours, including 1 hour to reach the target temperature. Afterward, the liberated HAs were acidified using the SAC resin and dried overnight at 80 °C–105 °C.

A total of 1.5 g calcium α-D-isosaccharinate with 98% purity was used as a standard both for the quantification of GISA in the HAs mixture and for the production of surfactant standards. The calcium α-D-isosaccharinate was dissolved in warm deionized water (DIW), and the solution was acidified to pH 2 using Amberlyst 15 SAC resin to liberate the corresponding GISA.

2.3 Synthesis of amide surfactants

For the synthesis of surfactants, approximately stoichiometric quantities of the reactants were employed, as the reaction is theoretically expected to proceed quantitatively due to the opposite polarity of the reagents. The HAs were used with no further purification, as it was noticed that the reaction was not inhibited by the presence of impurities. Initially, reactions were carried out using a pestle–mortar system. Subsequently, a few experiments were repeated in a ball mill to ensure the reproducibility and consistency of the results. The reaction scheme for the desired $GISA_L$ products is shown in Fig. 1.

In the pestle–mortar experiments, the dried hydroxy acids and amides were weighed and placed in a 250 mL mortar along with a small amount of water to facilitate a liquid-assisted grinding (LAG) reaction. The amount of liquid used was chosen so that the parameter λ was in the range between 0 and 1 mL $g_{reactants}^{-1}$. The exact amount was determined empirically, based on the ease of grinding the mixture in the mortar, as the open-air system allowed for continuous water evaporation. The mixture was ground for a total of 30 minutes, with 5 minutes allocated for cleaning the sides of the mortar. Intermediate samples were taken at 1-minute intervals during the first 15 minutes and at 5-minute intervals during the final 15 minutes. Both intermediate and final samples were analysed offline prior to drying.

For the ball mill experiments, a Retsch Planetary Ball Mill PM 200 equipped with a 250 mL stainless steel jar was used. The grinding media consisted of 400 g of 5 mm and 10 mm 316L steel balls. The rotary ball mill chamber and the grinding media were rinsed with ethanol prior to every reaction to ensure cleanliness. The reactants were weighed, and then the hydroxy acid mixture was dissolved in a certain amount of water to achieve a parameter λ around 0.75 mL $g_{reactants}^{-1}$. The ball mill was operated at 450 rpm and the time chosen was initially a total of 30 minutes. This consisted of a total of 15 minutes of grinding (3 times for 5 minutes), interspaced with 5-minute breaks for cooling.

For reactions involving hexadecyl and octadecyl amines in the ball mill, an alternative procedure was attempted. This involved a total reaction time of 30 minutes, comprised of 25 minutes of grinding with 5 intermediates 1-minute breaks for cooling. The adjustment was made based on the hypothesis that longer alkyl chains might require extended reaction times to achieve completion.

For the quantification of the synthetized surfactants, the reactions were also performed using the $GISA_L$ resulting from the calcium α-D-isosaccharinate salt as well as purchased lactic acid in the pestle–mortar equipment using reactants in stoichiometric quantities. The reactants were ground for 10 minutes plus a total of 5 minutes of intermediate breaks, and the products were used to create standards. All the reactions are summarised in Table 1 together with their conditions. In general, what is expected are reactions between the HAs with the amines.

2.4 Purification of surfactant mixtures

Recrystallisation with ethanol and methanol has been reported to be successful in many cases of surfactant purification.[46–48] In this work, the surfactants were dissolved in a minimum amount of ethanol followed by cooling, initially to room temperature and then in the fridge.

Silica gel gravity chromatography has also often been applied for lab-scale purification of surfactants.[49–51] For the

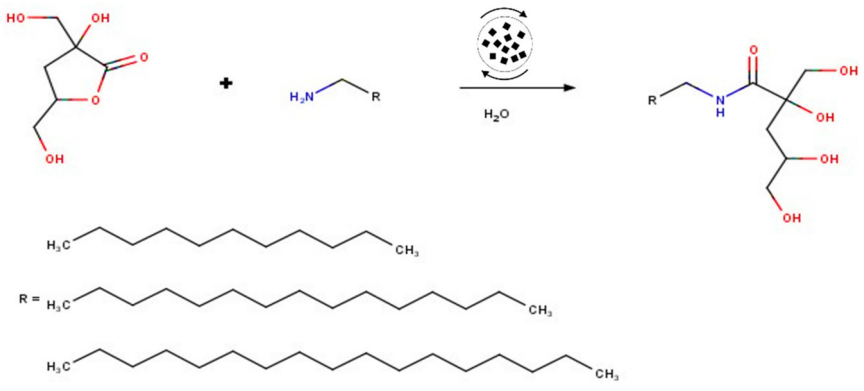

Fig. 1 Reaction scheme between $GISA_L$ and amides of different chain lengths.

Table 1 Summary of the performed reactions, raw material used and reaction conditions

Reaction name	λ [mL_{LAG} $g_{reactats}^{-1}$]	HAs	Amine	Equipment	Reaction time [min]	Speed [rpm]
MCC_12_PM	0.10	20 g MCC HAs	19.6 g 12-Amine	Pestle–Mortar	20 min monitored	—
MCC_16_PM	0.50	10 g MCC HAs	10.5 g 16-Amine			
MCC_18_PM	0.50	10 g MCC HAs	11.7 g 18-Amine			
ZFS_12_PM	0.50	0.48 g ZFS HAs	0.5 g 12-Amine	Pestle–Mortar	10	—
ZFS_16_PM	0.85	0.57 g ZFS HAs	0.6 g 16-Amine			
ZSF_18_PM	0.80	0.68 g ZFS HAs	0.8 g 18-Amine			
MCC_12_MILL15	0.75	20 g MCC HAs	13.2 g 12-Amine	Ball Mill	15	450
MCC_16_MILL15	0.75	10.4 g MCC Has	8.7 g 16-Amine			
MCC_18_MILL15	0.85	10.6 g MCC HAs	9.2 g 18-Amine			
MCC_16_MILL25	0.85	10 g MCC HAs	8.5 16-Amine	Ball Mill	25	450
MCC_18_MILL25	0.85	10.1 g MCC HAs	9 g 18-Amine			
LAC_12_PM	0.25	10 g LAC HAs	10 g 12-Amine	Pestle–Mortar	15	—
LAC_12_PM_1	0.08	6 g LAC HAs	6.9 g 12-Amine			
LAC_16_PM	0.33	3 g LAC HAs	3.1 g 16-Amine			
LAC_18_PM	0.45	3.2 g LAC HAs	3.5 g 18-Amide			
GISA_STN_12	0.50	0.3 g $GISA_L$	0.33 g 12-Amine	Pestle–Mortar	10	—
GISA_STN_16	0.60	0.3 g $GISA_L$	0.44 g 16-Amine			
GISA_STN_18	0.70	0.3 g $GISA_L$	0.5 g 18-Amine			
LA_STN_12	0.27	1.2 g LA	2.47 g 12-Amine	Pestle–Mortar	10	—
LA_STN_16	0.56	1.2 g LA	3.2 g 16-Amine			
LA_STN_18	0.62	1.2 g LA	3.5 g 18-Amine			

reactions involving dodecyl amine products, purification was conducted in isocratic mode using a 1 : 1 hexane : isopropanol solvent system for a total of 5 bed volumes (BV). For the reaction mixtures of hexadecyl and octadecyl amides, it was performed in gradient mode (hexane: iPrOH, 1 BV 1 : 1, 1 BV 2 : 1, 1 BV 1 : 0, 1 BV 1 : 1, 1 BV 1 : 2, 1 BV 0 : 1). The reactions were carried out in a column (ST/NS 24/40, I.D. × L 20.0 mm × 305 mm) and 0.1 BV of 100 g L^{-1} feed was used for every experiment.

Foam fractionation exploits the capability of surface-active compounds to accumulate at an interface and form foams. The setup is shown in Fig. 2 and consists of a flowmeter to regulate the compressed air flow connected to the bottom of an empty column (ST/NS 24/40, I.D. × L 20.0 mm × 305 mm) equipped with a frit which acts as an air sparger to generate small bubbles. The surfactant paste was dissolved in deionised water at a concentration of approximately 20 g L^{-1} and poured into the column. The air flow was then set to 0.05 nL min^{-1}, and the valves were opened. The foam formed gradually, allowing the drainage of excess liquid. The system is operated in batch mode, where a pool of crude surfactant solution is left to foam until the concentration of surfactants in the pool is too low for foam formation. The foam is collected manually and left to collapse and dry.

2.5 Chemical analyses

An HPLC–DAD Agilent 1200 Series was used to monitor the reactions and for quantitative analysis. A UPLC–TOF–MS Waters Acquity–LCT Premier XE was used in negative polarisation mode for the recognition of the species though mass analysis.

The HAs were analysed using an Agilent Luna Omega Polar C18 column (5 μm, 250 × 4.6 mm) in isocratic mode. The mobile phase consisted of 0.1% H_3PO_4 and 50 mM NaH_2PO_4

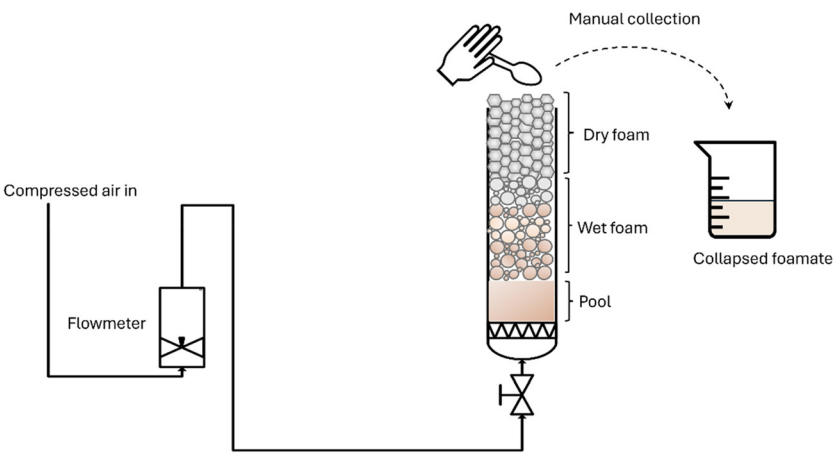

Fig. 2 Foam fractionation setup used for the purification of surfactant mixtures.

in water, with flow rates of 0.5 mL min^{-1} in the HPLC–DAD and 0.4 mL min^{-1} in the UPLC–TOF–MS.

For surfactant analysis, an InfinityLab Poroshell 120 EC–C18 column (3.0 × 100 mm, 2.7 μm) was used coupled with a guard column (InfinityLab Poroshell 120 EC–C18 HILIC–Z, 2.1 × 5 mm, 2.7 μm). The mobile phase consisted of a mixture of acetonitrile (ACN) and water (60 : 40) with 0.1% formic acid (FA), and the flow rates were maintained at 0.5 mL min^{-1} in the HPLC–DAD and 0.4 mL min^{-1} in the UPLC–TOF–MS. Both the HPLC–DAD and UPLC–TOF–MS systems employed the same columns and methods for analysis.

For the structural characterisation of surfactants, NMR, JEOL JNM–ECZ–500R 500 MHz, was used (Tampere University). For this, the samples were dried and dissolved in DMSO–D_6.

2.6 Characterisation of surfactant behaviour in solution

Surfactants' key properties to study include their ability to foam, emulsify, and form suspensions, as these are closely related to the solubility and interfacial activity of the molecules. Commonly used parameters to describe surfactant behaviour in solution include the critical micelle concentration (CMC), hydrophilic lipophilic balance (HLB) and the partition coefficient (K_P). Additionally, qualitative experiments can be conducted to assess the surfactants' emulsifying and foaming capabilities.

Surface tension and CMC. For the estimation of the CMC, measurements were done using a contact angle goniometer, which is a device capable of performing different types of optical measurements, including the pendant drop and sessile drop techniques. The software associated with the contact angle goniometer is able to optically collect data and fit them in the Young–Laplace equation which relates the curvature radius of the droplet to the surface tension and the Laplace pressure. For comparison, the commercial surfactant sorbitan laurate was tested under identical experimental conditions. Additionally, the results were compared with literature data for methyl glucamides (MEGA), as their great structural similarity to GISA–amides provides a relevant benchmark.

The pendant drop experiments were used to measure the surface tension change with concentration. A series of 10 μl droplets of increasing surfactant concentration solutions was ejected through a syringe. The elongation of the pendant drop was proportional to the decrease in surface tension. The elongation proceeded until the CMC was reached. The pendant drop experiments were conducted with surfactant concentrations ranging from 0 to 5 mM at a temperature of 20 °C.

A similar measurement was done with the sessile drop. The drop had a certain contact angle at the three-phase contact point related to the surface tension through the Young equation. The experiments consisted of depositing 10 μl droplets with concentrations from 0 to 5 mM on a well-defined hydrophobic surface using a syringe at a temperature of 20 °C, carefully rinsing the surfaces with EtOH after every drop. Two different materials were used, polypropylene and polystyrene. This, in addition to providing understanding of the wetting properties of the surfactants, was done to have differentiated data to provide more accuracy.

Hydrophilic–lipophilic balance (HLB). The hydrophilic–lipophilic balance (HLB) is generally estimated using the Griffin method[52] and the Davies method.[53] The Griffin method is purely based on the molecular structure of the surfactant, and it is calculated as follows (eqn 1).

$$\mathrm{HLB_{Griffin}} = 20 \cdot \frac{\mathrm{MW_{Hydrophilic}}}{\mathrm{MW_{Surfactant}}} \quad (1)$$

The Davies method[53] is an empirical method which evaluates the HLB by considering the balance of the sizes and strengths of the hydrophilic and lipophilic moieties of a surfactant molecule. To each group, the Davies method assigns a group number, evaluated based on the activity coefficients (eqn 2).

$$\mathrm{HLB_{Davies}} = 7 + \sum n\mathrm{H_{hydrophiles}} - \sum m\mathrm{H_{lipophile}} \quad (2)$$

Here, n is the number of times a certain hydrophilic group is present in the molecule, while m is the number of times a certain lipophile is present. These values are widely available in the literature, and, hence, they are not reported here.[53,54] Other methods have been also developed to overcome the limitations of the previous two. For example, the Chemaxon method developed by the software provider is a consensus method based on the Davies and Griffin methods.[55] These values can be calculated manually or using software for more rigorous results. Here, the calculations were done using the software MarvinSketch from Chemaxon.

Partition coefficient *K*. The partition coefficient K was also estimated as in eqn (3).

$$K = \frac{C^{\mathrm{surf}}_{\mathrm{Oil}}}{C^{\mathrm{surf}}_{\mathrm{Water}}} \quad (3)$$

K is the ratio of the concentrations of a compound in two immiscible solvents, *i.e.*, water and an oil, at equilibrium, and it is usually reported in terms of $\log K$. Most commonly, the partition coefficient is evaluated in a system where one of the solvents is water, while the second is 1-octanol. The K_{OW} can be predicted based on the molecular structure by interpolating the values of $\log K_{WO}$ of compounds with similar structures. In this case, MarvinSketch was used for the prediction of K_{OW}. The software offers two methods for estimation: the Chemaxon method is based on Chemaxon's own $\log K_{WO}$ model for a water–octanol system, which is based on the VG method (derived from Viswanadhan *et al.*[56]), while the Consensus method is based on the model built by Chemaxon, that of Klopman *et al.*,[57] and the PhysProp database. Since these methods could lead to substantial errors, it was worth using another software program, ChemSketch by ACD Labs, to obtain an average value of the coefficient. The same programmes were used to also estimate the values of the partition coefficients for the commercial surfactants with similar structure, *i.e.*, sorbitan laurate and the methyl glucamides. When

available in the literature, experimental values are also reported.

For the $GISA_L$ products, which are the main target compounds, experimental values were obtained by contacting the phases for a long time to reach equilibrium without shaking to avoid the formation of emulsions. In this case, 1% (w/w) surfactant solutions were contacted with octanol for three days, and then the two phases were measured using HPLC.

Foam height and stability experiments. For the estimation of the foaming capabilities of surfactants, a type of static foam test consists in shaking a solution of surfactant followed by foam height measurements. Similarly, as done by Campana *et al.*,[58] 10 mL of 0.1% w/w solution was put in a 100 mL graduated cylinder and shaken with a vertical shaker for 30 seconds. The foam was measured and monitored for several days. Also, in this case, the experiment was repeated for sorbitan laurate.

Emulsion stability experiments. To test the surfactants' capabilities of stabilising emulsions, different water/oil ratios and surfactant percentages were tried. The conditions are reported in Table 2. The preparation method was the same for all experiments. The two phases were heated to 50 °C, the continuous phase was vigorously stirred with a magnetic stirrer at 1600 rpm, and then the dispersed phase was added gradually. The obtained emission was left to set for some hours and, then, if stable, a drop was added to a beaker filled with water to verify the type of emulsion. Thickening/gelling capabilities were also observed by subjecting a 1% surfactant solution to heating and cooling cycles. The same emulsion experiments were also performed with sorbitan laurate.

3. Results and discussion

3.1 Hydroxy acids production

The compositions of the hydroxy acids obtained by alkaline digestion of various raw materials are reported in Table 3. The digestions of lactose and microcrystalline cellulose (MCC) were done using relatively lower temperatures with the aim of obtaining HA mixtures with a high percentage of GISA and a minor quantity of other acids at the cost of lower conversion rates. In fact, increasing the temperature promoted the production of low molecular weight acids. For the digestion of ZFS, instead, a higher temperature was used to ensure enough acids would be produced, since the raw material was very low grade.[10] Only the acids for which standards were available could be certainly identified, namely, glycolic acid, 2,5-DHPA, 2-HBA, formic acid, acetic acid, lactic acid and GISA with its lactone. The aim of this synthesis was to produce a hydroxy acid mixture chemically similar to processed industrial black liquor (after delignification and the removal of pulping chemicals). Sodium hydroxide could, in principle, be recovered from the SAC resin during the regeneration process, but it is not within the scope of the research.

Table 3 Composition of the dried HA mixtures from different sources

Compound	MCC [g g^{-1}]	ZFS [g g^{-1}]	Lactose [g g^{-1}]	Calcium D-isosaccharinate [g g^{-1}]
Glycolic acid	0.009	0.014	0.011	—
GISA lactone	0.663	0.435	0.596	0.81
2,5-DHPA	0.044	0.008	0.008	—
2-HBA	0.005	0.062	0.021	—
Formic acid	0.008	0.039	0.007	—
α-GISA	0.004	0.047	0.062	0.088
Acetic acid	0.014	0.023	0.012	—
Lactic acid	0.015	0.053	0.013	—
$(C_xH_yO_z)_{176}$	0.098	NQ	0.031	—
$(C_xH_yO_z)_{178}$	0.072	0.188	0.037	—
$(C_xH_yO_z)_{192}$	0.027	NQ	NQ	—
2-HGA	0.033	0.026	0.038	—
Conversion	45%	—	47%	—
Yield	67%	51%[a]	72%	97%

NQ: not quantifiable. [a] Yield refers to cellulose which is 60% of the mass of the ZFS.

For the other compounds, hypotheses could be made according to the mass identified *via* UPLC–MS and literature data.[59] The chromatogram of the HAs and their spectrum are reported in Fig. 3 and ESI Fig. S1.† The conversion of the digestions was calculated in terms of produced acids (unreacted base), which is a measure of how much of the cellulose was converted into Has; this was evaluated by titrating the alkaline solution with HCl. The yield was evaluated in terms of GISAs over total recognised acids.

Four compounds with masses around 147, 176, 178 and 192 g mol^{-1} (indicated in Table 3 as $(C_xH_yO_z)_{MW}$) were particularly worthy of attention. These four molecules could indeed be associated with some polycarboxylic acid or hydroxycarboxylic acid, as they reacted with the amines to form amide by-products (see Tables 5–7). Käkölä *et al.*[60] identified a compound with mass 147 g mol^{-1} as 2-hydroxyglutaric acid (2-HGA). Niemelä *et al.*[59] made an extensive study of the hundreds of different acids that can be found after the alkali treatment of cellulose; several compounds with compatible masses for each of these were listed, but it was not possible to isolate these compounds to conduct a structural evaluation.

Table 2 Phases involved in the emulsification experiments

Continuous phase	Dispersed phase	Surfactant
50% water	50% octanol	0.5% total weight of 12,16,18-GISA-Amide/sorbitan laurate
90% water	10% sunflower seeds oil	1% total weight of 12,16,18-GISA-Amide/sorbitan laurate
90% sunflower seeds oil	10% water	1% total weight of 12,16,18-GISA-Amide/sorbitan laurate
80% water	20% sunflower seeds oil	2% total weight of 12,16,18-GISA-Amide/Sorbitan laurate

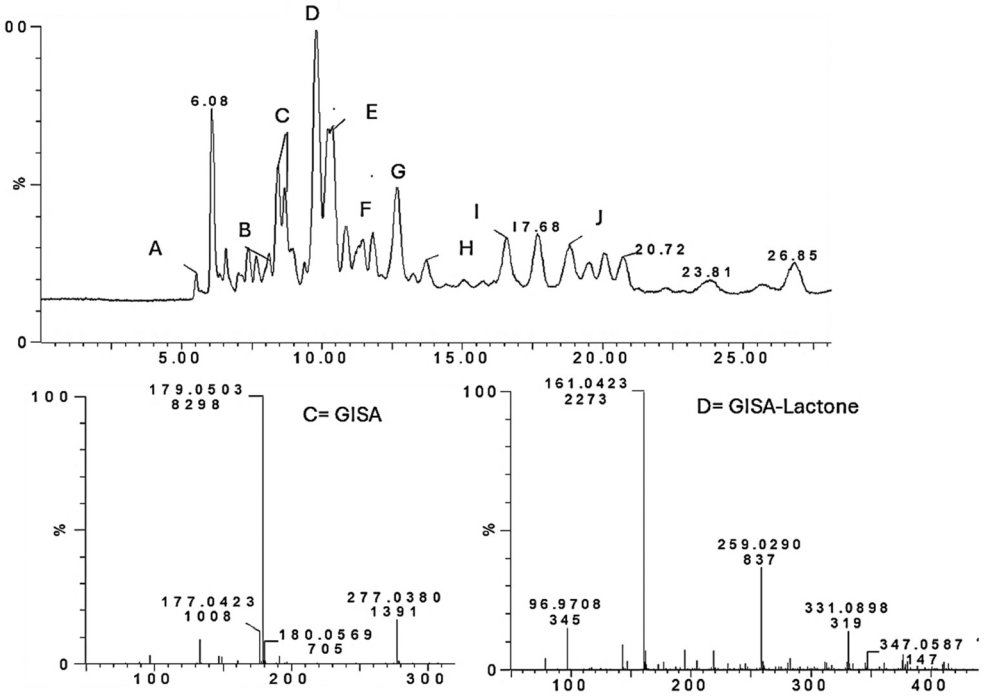

Fig. 3 UPLC MS chromatogram and spectrum of HA mixture from MCC. A = $(C_xH_yO_z)_{176}$, B = glycolic acid, C = GISA, D = GISA-lactone, E = $(C_xH_yO_z)_{178}$, lactic acid + formic acid, F = acetic acid + formic acid, G = 2,5-DHPA, H = $(C_xH_yO_z)_{192}$, I = 2-HGA, and J = 2-HBA. The other spectra are available in ESI Fig. S1.†

3.2 Synthesis of amide surfactants

Table 4 reports the identifiable products for each reaction together with their monoisotopic mass and IUPAC name. The compounds listed in Table 4 were subjected to structural characterisation with carbon and proton NMR. The resulting NMR data are reported only once for the GISA and lactic amides, as the size of the alkyl chain only influences the dimension of the signal relative to that part of the molecule (δ 1.19 ppm).

GISA–amides: ^{1}**H NMR** (500 MHz, DMSO–D_6) δ 7.53 (br s, J = 6.0 Hz, 1H, NH), 5.20 (br s, 1H, OH), 3.61 (dp, 1H, CH(OH)), 3.45 (dd, 2H, O═CC(OH)CH_2OH), 3.30 (dd, 2H HOCH_2CH(OH)CH_2), 2.99 (dd, 2H, CH_2NH), 2.73–2.66 (m, 1H, CH_2OH), 1.67–1.52 (m, 2H, HOCH_2CH(OH)CH_2), 1.37–1.29 (m, 2H, CH_2CH_2NH), 1.19 (alkyl CH_2), 0.81 (t, J = 6.8 Hz, 3H, CH_3). ^{13}**C NMR** (126 MHz, DMSO–D_6) δ 174.57(C═O), 77.35 (C(OH)COH), 69.06 C(OH)COH, 68.64 (HOCH_2CH), 68.26 (HOCH_2CH), 67.74, 66.97 (OHCCH_2C(COH)OH), 38.95 (NHCH_2), 31.84–26.38 (alkyl CH_2), 22.65 (CH_2CH_3), 14.51 (CH_3). **Lactamides:** ^{1}**H NMR** (500 MHz, DMSO-D_6) δ 7.63 (br s, J = 6.0 Hz, 1H, NH), 3.88–3.54 (O═CCHCH_3OH), 3.03–2.65 (CH_2NH), 1.47 (CH_2CH_3), 1.28–1.20 (m, 2H, CH_2CH_2NH), 1.21–1.07 (alkyl CH_2), 0.81 (3H CH_3).^{13}**C NMR** (126 MHz, DMSO-D_6) δ174.76 (C═O), 67.76 (O═CHCH_3OH), 39.32 (CH_2NH), 31.84–26.41 (alkyl CH_2), 22.65 ($CH_2CH_2CH_3$), 14.50 (CH_2CH_3).

The presence of the amide bond is proven by the amide –NH shift δ 7.53 ppm and δ 7.63 ppm in the ^{1}H NMR and from the COO– shift in the ^{13}C NMR at δ 174.76 ppm. The NMR spectra are reported in the ESI Fig. S7–S18.†

The compositions of the resulting amidation reactions are reported in Tables 5–7. All the concentrations are evaluated based on the 12-GISA-Amide standard except for the lacta-

Table 4 Products that can be identified with standards

Product	R group[a]	IUPAC name	Monoisotopic mass [g mol^{-1}]
12-GISA-amide	C11H24	*N*-Dodecyl-2,4,5-trihydroxy-2-(hydroxymethyl) pentanamide	347.27
16-GISA-amide	C15H32	*N*-Hexadecyl-2,4,5-trihydroxy-2-(hydroxymethyl) pentanamide	403.33
18-GISA-amide	C17H36	*N*-Octadecyl-2,4,5-trihydroxy-2-(hydroxymethyl) pentanamide	431.36
12-Lactamide	C11H24	*N*-Dodecyl-2-hydroxypropanamide	257.24
16-Lactamide	C15H32	*N*-Hexadecyl-2-hydroxypropanamide	312.29
18-Lactamide	C17H36	*N*-Octadecyl-2-hydroxypropanamide	340.32

[a] Refer to Fig. 1.

Table 5 Resulting compositions of the reactions involving dodecyl amine and the HAs mixtures from different sources

Reaction name	12-GISA-Amide ($g\ g^{-1}$)	12-($C_xH_yO_z$)$_{176}$-Amide ($g\ g^{-1}$)	12-($C_xH_yO_z$)$_{178}$-Amide ($g\ g^{-1}$)	12-($C_xH_yO_z$)$_{192}$-Amide ($g\ g^{-1}$)	12-HGA-Amide ($g\ g^{-1}$)	12-Lactic amide ($g\ g^{-1}$)	Max yield, η_{max}	Yield %, $\eta_{\%}$
MCC_12_PM	0.540	0.058	0.076	0.075	0.014	0.007	0.72	75
ZFS_12_PM	0.382	NQ	0.110	0.098	0.021	0.087	0.54	70
MCC_12_MILL	0.379	0.010	0.062	0.061	0.005	0.022	0.86	44
LAC_12_PM	0.733	0.027	0.020	0.025	0.013	0.029	0.83	88
LAC_12_PM_1	0.558	0.008	0.015	0.015	0.011	0.012	0.67	83
GISA_STN_12	0.879	—	—	—	—	—	0.97	90
LA_STN_12	—	—	—	—	—	0.75	1	75

Table 6 Resulting compositions of the reactions involving hexadecyl amine and the HAs mixtures from different sources

Reaction name	16-GISA-Amide ($g\ g^{-1}$)	16-($C_xH_yO_z$)$_{176}$-Amide ($g\ g^{-1}$)	16-($C_xH_yO_z$)$_{178}$-Amide ($g\ g^{-1}$)	16-($C_xH_yO_z$)$_{192}$-Amide ($g\ g^{-1}$)	16-Lactic amide ($g\ g^{-1}$)	16-HGA-Amide ($g\ g^{-1}$)	Max yield η_{max}	Yield % $\eta_{\%}$
MCC_16_PM	0.539	NQ	0.092	0.080	0.093	0.038	0.81	67
ZFS_16_PM	0.376	NQ	0.048	0.121	NQ	0.043	0.63	60
MCC_16_MILL15	0.437	0.015	0.050	0.080	NQ	NQ	0.90	49
MCC_16_MILL25	0.370	0.012	0.031	0.046	NQ	NQ	0.90	41
LAC_16_PM	0.448	0.008	0.010	0.014	0.007	NQ	0.79	57
GISA_STN_16	0.857	—	—	—	—	—	0.90	95
LA_STN_16	—	—	—	—	0.66	—	1	66

Table 7 Resulting compositions of the reactions involving octadecyl amine and the HA mixtures from different sources

Reaction name	18-GISA-Amide ($g\ g^{-1}$)	18-($C_xH_yO_z$)$_{176}$-Amide ($g\ g^{-1}$)	18-($C_xH_yO_z$)$_{178}$-Amide ($g\ g^{-1}$)	18-($C_xH_yO_z$)$_{192}$-Amide ($g\ g^{-1}$)	18-Lactic amide ($g\ g^{-1}$)	16-HGA-Amide ($g\ g^{-1}$)	Max yield, η_{max}	Yield %, η%
MCC_18_PM	0.359	NQ	0.009	0.019	NQ	0.020	0.80	45
ZFS_18_PM	0.320	NQ	NQ	NQ	NQ	NQ	0.56	57
MCC_18_MILL15	0.778	NQ	0.026	0.058	0.082	0.024	0.92	85
MCC_18_MILL25	0.323	NQ	NQ	NQ	NQ	NQ	0.87	37
LAC_18_PM	0.278	NQ	NQ	NQ	NQ	NQ	0.82	34
GISA_STN_18	0.637	—	—	—	—	—	0.88	72
LA_STN_18	—	—	—	—	0.54	—	1	54

mides products that are evaluated based on the 12-lactamide standard. This was done since the alkyl chain length has no relevant impact on the DAD response.

The maximum yield represents the maximum amount of surfactant that can be obtained if all the GISA present in the given HAs mixture reacts with one molar equivalent of the amine, and it is evaluated as in eqn (4):

$$\eta_{max} = \frac{m_{GISA} + m_{amine}}{m_{tot\ reactants}} \quad (4)$$

where m_{GISA} is the mass of GISA in the HAs, calculated as the mass fractions (from Table 3) multiplied by the mass of the used HAs mixture (from Table 1), while m_{amine} corresponds to 1 molar equivalent of amine to the amount of GISA their sum is the maximum amount of amide that can be produced. The $m_{tot\ reactants}$ is the sum of the HAs mixture and amine used in the reaction (Table 1).

The percentage yield is calculated as in eqn (5):

$$\eta_{\%} = \frac{\eta_{amide}}{\eta_{max}} \times 100 \quad (5)$$

where η_{amide} is the actual yield, which correspond to the values reported in Tables 5–7 in terms of $g_{GISA\text{-}amide}\ g_{mixture}^{-1}$. In Table 5 are reported the resulting composition of the surfactant mixtures involving the HAs from different sources and the dodecylamine as alkyl chain.

In Fig. 4 are reported the chromatogram and the mass spectra of the identified species for the reaction MCC_12_PM. The first peak eluting at 1.23 min represents the unreacted starting material, both the leftover HAs and the protonated amines which have very weak interaction with the column. The main product (12-GISA-Amide) is reported in Fig. 4, peaks A and B together with the complex formed with bromine and formic acid. Other amide products were also formed, namely,

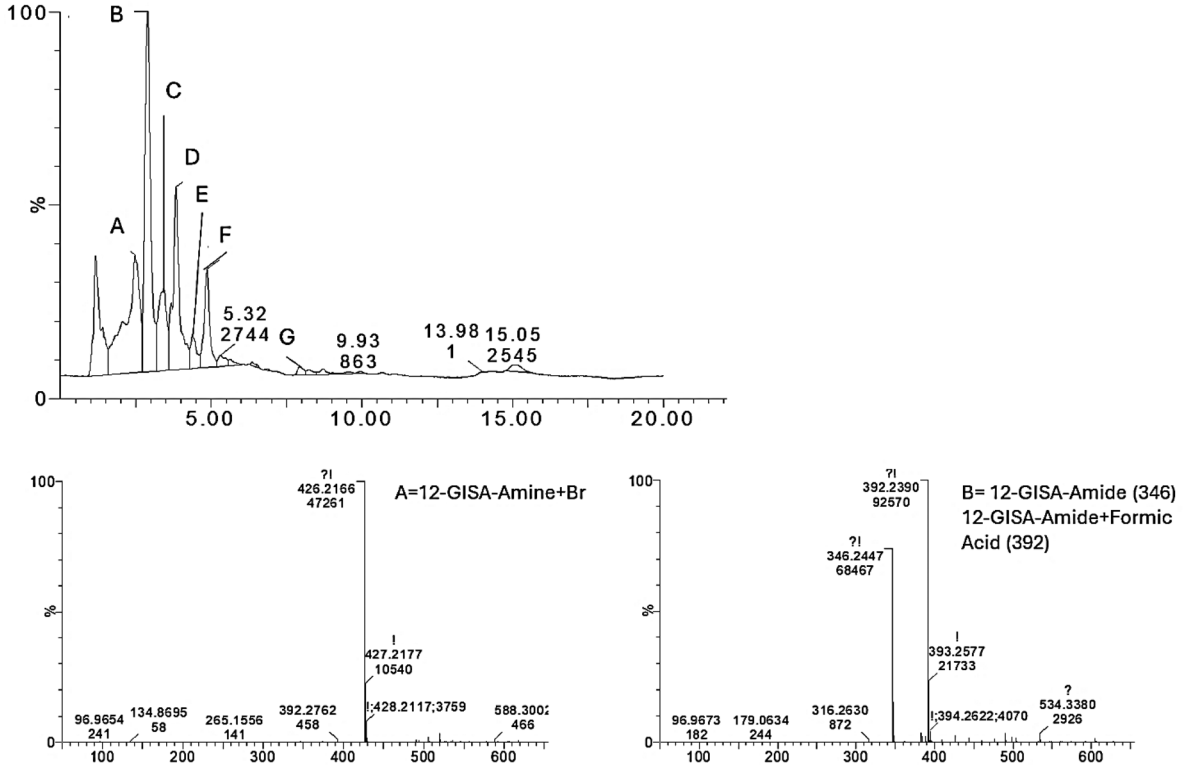

Fig. 4 UPLC–MS chromatogram and mass spectra for reaction MCC_C12_PM. A = 12-GISA-Amide + Br, B = 12-GISA-Amide + formic acid, C = 12-$(C_xH_yO_z)_{176}$-Amide + formic acid, D = 12-$(C_xH_yO_z)_{178}$-Amide, E = 12-2-HGA-Amide, F = 12-$(C_xH_yO_z)_{192}$-Amide, and G = 12-lactamide. The spectra for the other compounds can be seen in ESI Fig. S2.†

the 12-$(C_xH_yO_z)_{176}$-, 12-$(C_xH_yO_z)_{178}$- and 12-$(C_xH_yO_z)_{192}$-Amide, as shown in Fig. 4 peaks C, D and F, respectively, while E is the 12-HGA-amide and G the 12-lactamide. The spectra of these molecules are reported in ESI Fig. S2.†

For the reactions involving hexadecyl amines, reported in Table 6, and octadecyl amines, in Table 7, extensively long times for the UPLC–MS analysis would have been necessary, hence some of the compounds were not identified in those measurements since the device was not readily available to repeat the analysis. What was done instead, was to synthesize standards for the lactamide which is the last compound to elute and then compare the intermediate peaks with those identified for the dodecylamide products, since the elution order should be maintained. In Table 6 are reported the composition of the reactions involving hexadecyl amine as alkyl chain.

Fig. 5 displays the UPLC–MS analysis in terms of the chromatogram and mass spectra, in which it was possible to recognise the peak containing the unreacted starting material (peak at 1.17) and the main product peaks A and B. The 16-$(C_xH_yO_z)_{178}$- and the 16-$(C_xH_yO_z)_{192}$-Amides are visible in Fig. 5 as peaks C and E, respectively. It was also possible to identify the product of HGA as peak I. The mass spectra for these compounds are reported in ESI Fig. S4.† However, the measurement was too short to identify the 16-lactamide, which was later measured using HPLC. The chromatograms for the HPLC measurements for the lactamide standard (LA_STN_16) and MCC_16_PM can be found in ESI Fig. S3.†

Finally, Fig. 6 shows the chromatogram and the spectra obtained from the UPLC–MS analysis of the reactions of MCC_18_PM (top) and ZFS_18_PM (bottom); analogously, the peak at 1.17 min represents the unreacted starting materials. It was possible to identify 18-GISA-Amide in Fig. 6 as peaks A and B, 18-HGA-Amide as peak C and 18-$(C_xH_yO_z)_{178}$-Amide as peak D. The mass spectra for these compounds can be found in ESI Fig. S6.† The side-products 18-$(C_xH_yO_z)_{176}$-Amide and 18-$(C_xH_yO_z)_{192}$-Amide were not found in these analyses but can be identified in the HPLC together with 18-lactamide, also not detected here since the measurement time was not broad enough. The HPLC chromatograms are reported in ESI Fig. S5.†

In summary, from the results of the analyses, it can be seen that the reaction proceeds with relatively good yields even in the presence of high percentages of impurities. The difficulties of detecting some of the species of longer chain length is due both to the lower yield with respect to dodecyl amine, which results in undetectable quantities, and also intrinsically to the analysis method. The chromatographic column used here is a modified C18 type, which has a particular affinity for C16 and C18 compounds, resulting in very strong interactions and very long retention times, up to almost two hours for 18-lactamide.

It is also interesting to notice that the parameter λ plays an essential role in the reaction conversion as well as the chain

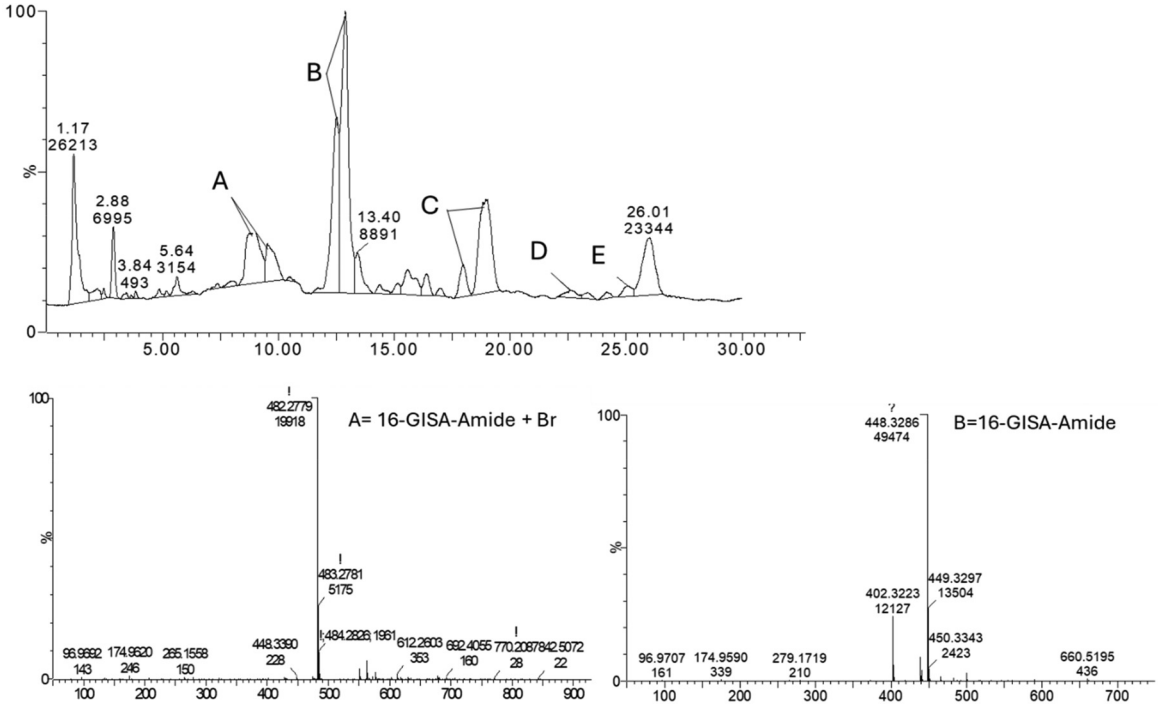

Fig. 5 UPLC–MS chromatogram and mass spectra for reaction MCC_C16_PM. A = 16-GISA-Amide + Br, B = 16-GISA-Amide, C = 16-$(C_xH_yO_z)_{178}$-Amide, D = 16-HGA-Amide, and E = 16-$(C_xH_yO_z)_{192}$-Amide. The spectra for the other compounds can be seen in ESI Fig. S4.†

length of the amine. In Table 5, for example, it can be seen that, for a chain length of 12, increasing the water content (MCC_12_PM and MCC_12_MILL15) inhibited the reaction, drastically reducing the yield. On the other hand, looking at Table 7, it can be seen that, by increasing λ for a chain length of 18, the reaction yield increased significantly (MCC_18_PM and MCC_18_MILL15). Looking at Table 6, the yield decreased when increasing the water content (MCC_16_PM and MCC_16_MILL15). These experiments also have another major difference, *i.e.*, MCC_12_PM, MCC_16_PM, and MCC_18_PM were done in a pestle–mortar system and hence subjected to inconsistencies, while MCC_12_MILL, MCC_16_MILL and MCC_18_MILL was performed in the ball mill with the exact same procedure. Here, what is crucial is that, since the reaction happens thanks to mechanical stimuli, it is essential to add to the system an appropriate quantity of liquid so that the paste is not so thick that it inhibits the reaction and stops the molecular diffusion and phase contacting, as happened in MCC_18_PM. At the same time, excessive water, like in MCC_12_MILL and MCC_16_MILL, makes the reaction mixture too fluid, so that the friction applied and the mechanical energy transferred to the molecules were not enough. Another important data point that can be extrapolated from Tables 6 and 7 is that when the reaction time is increased and the cooling time reduced, the yield of the reaction is decreased (MCC_16_MILL15 *vs.* MCC_16_MILL25 and MCC_18_MILL15 *vs.* MCC_18_MILL25). In fact, when the reaction mixture is ground in the ball mill, the reacting mixture is heated, and this has the major effect of melting the reactants with the consequent reduction of their viscosity, which diminishes the mechanical energy transferred to the molecules. As a result, longer reaction times are not necessary and can actually make the yield worse if there is not proper cooling.

3.3 Purification of surfactant mixtures

Purification was done on the mixtures produced in reactions MCC_12_PM, MCC_16_PM and MCC_18_PM, and the results are reported in Table 8. As expected, silica gel chromatography allows the achievement of high purity; however, it is limited to laboratory scale and involves intensive use of solvents such as hexane. For recrystallisation in EtOH, multiple slow steps are needed to reach good purity; however, it is not possible to completely remove the unreacted amines. In addition, this method did not work well with MCC_12_PM, as the compounds were too soluble and the process slow. However, this method can be scaled up and uses a green solvent that can be recirculated. Foam fractionation showed promise and only involves the use of water and air flow. Already, this simple setup was sufficient to relevantly increase the purity; more complex and specific setups could significantly improve the efficiency of this process.

3.4 Critical micelle concentration (CMC)

Before proceeding with the evaluation of the surfactant solutions, the device was tested with water for accuracy. The measured water surface tension was 75.6 ± 1.0 mN m^{-1}, while the value reported in literature is 74 mN m^{-1}. The measured contact angle between water and the polypropylene surface

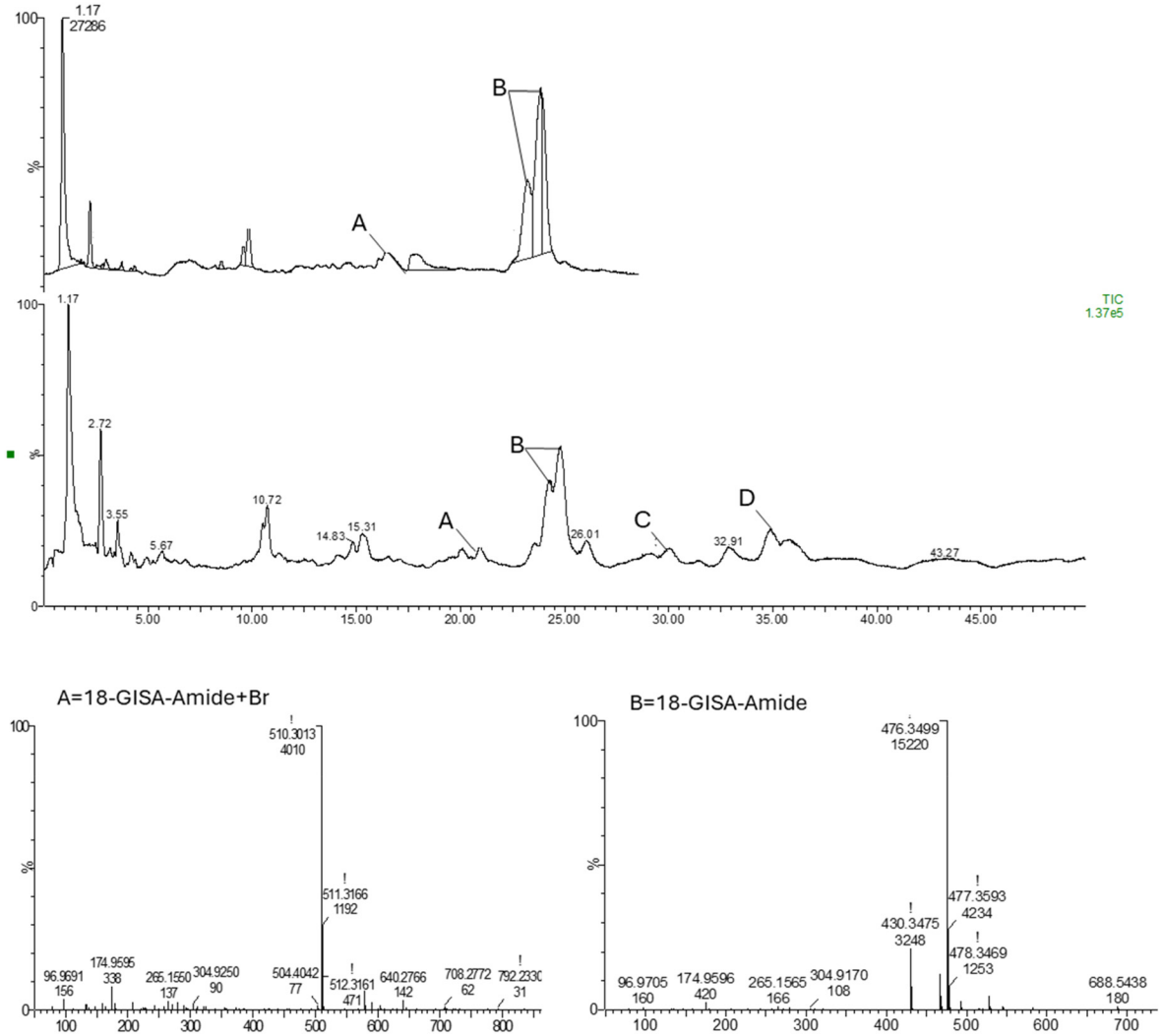

Fig. 6 Chromatogram and mass spectra for reactions of MCC_18_PM (top) and ZFS_18_PM (bottom). A = 18-GISA-Amide + Br, B = 18-GISA-Amide, C = 18-HGA-Amide, and D = 18-$(C_xH_yO_z)_{178}$-Amide. The spectra for the other compounds can be seen in ESI Fig. S6.†

Table 8 Results from different purification techniques applied to MCC_12_PM, MCC_16_PM and MCC_18_PM

Purification technique	Max purity for C12 [g g^{-1}]	Max purity for C16 [g g^{-1}]	Max purity for C18 [g g^{-1}]
Gravity silica gel chromatography	0.91	0.98	0.85
Recrystallisation in EtOH	—	0.88	0.56
Foam fractionation	0.75	0.69	0.46

was 85.5° ± 6.0° and that for polystyrene was 101° ± 1°, while the values found in literature were respectively 87.4° and 102°. The critical micelle concentrations (CMC) were calculated from the cross point of the contact angle *versus* concentration lines in the sessile drop experiments, as well as the cross point of the surface tension *versus* the logarithm of concentration in the pendant drop experiments. The values of CMC are reported in Table 9, and they are expressed in terms of mean value and their PLS error among the duplicates. The values obtained are in agreement with the generally observed trend in surfactants and are comparable with those of similar surfactants. In fact, the CMC decreases with increasing chain length, as the hydrophobic interactions, described as van der Waals forces, become more favourable at longer chain lengths; this conformation minimises the unfavourable contact of the chains with water and lowers the energy of micellization. In addition to the CMC, the values of the surface tension at CMC are reported. These surfactants are capable of lowering the surface tension of water from 74 mN m^{-1} to 27, 31 and 34 mN m^{-1}, respectively, with increasing chain length.

Table 9 also reports the values of the Langmuir isotherm at CMC, Γ_{CMC}, which indicates the moles of surfactants covering the water–air interface, called surface excess. These values have the meaning of an absorbed monolayer at the water–air interface. The value Γ_{CMC} is defined as in eqn (6)

Table 9 Experimental physical–chemical properties of the GISA–Amide surfactants

Surfactant	γ@CMC	Γ@CMC [10^{-6} mol m^2]	a_m@CMC [Å^2]	CMC [mM], Pendant drop	CMC [mM], Sessile drop	Mean [mM]
12-GISA-Amide	27	7.8	21	0.767 ± 0.1	PS: 0.793 ± 0.042 PP: 0.732 ± 0.034	0.760
16-GISA-Amide	31	8.6	19	0.034 ± 0.005	PS: 0.035 ± 0.001 PP: 0.030 ± 0.001	0.033
18-GISA-Amide	34	9.2	18	0.016 ± 0.002	PS: 0.010 ± 0.002 PP: 0.0095 ± 0.003	0.012
Sorbitan laurate	27	9.4	18	0.032	PS: 0.041 ± 0.005 PP:0.048 ± 0.006	0.044
Surfactant	*γ@CMC*	Γ@CMC	a_m@CMC	CMC		
Sorbitan laurate	28[a 62]	4.1[a 61]	40[a 61]	0.02–0.06[a 61]		
MEGA-12	30[a 63,64]	4.1[a 63,64]	40[a 63,64]	0.35[a 63,64]		
MEGA-14	36[a]	4.7[a]	35[a]	0.014[a]		

[a] Literature values, measured with surface tensiometer.

$$\Gamma_{CMC} = -\frac{1}{RT}\frac{\Delta\gamma}{\Delta \log C} \quad (6)$$

where $\frac{\Delta\gamma}{\Delta \log C}$ is the slope of the line in the pre-micellar regime in the graph γ *versus* log C, as reported in Fig. 7, and it is possible to compare the trends and CMC for the three GISA surfactants.

The CMC is one of the most important values when describing the physicochemical characteristics of surfactants. From a theoretical point of view, it represents the thermodynamic state in which molecules arrange to minimise the Gibbs free energy of the system. Practically, it represents the minimum concentration at which a surfactant in solution is able to form micelles. Surfactants behave very differently when their concentration is above the CMC in terms of solubility, refractive index, surface tension, molar conductivity, osmotic pressure, *etc*. In fact, below the CMC, surfactants are present as single molecules in solution or at the air–water interface. Hence, these values can be interpreted as the lower concentration limit of applicability. The values of CMC tend to decrease with temperature.

Another datum reported in Table 9 is the area occupied by a surfactant molecule at CMC, a_m, *i.e.*, in the monolayer. This value is a measure of the packing capability of the surfactant. It is evaluated as in eqn (7):

$$a_m = \frac{1}{\Gamma_{CMC} N_A} \quad (7)$$

where Γ_{CMC} is the surface concentration and N_A is Avogadro's number. The area occupied by a surfactant molecule decreases, counterintuitively, with increasing chain length. This is due to the tighter packing of the surfactant with longer chain length, in which the hydrophobic interactions are predominant and, hence, their position at the interface with air is more favourable. For this reason, more molecules accumulate at the interface, resulting in less space for each molecule.[65] For the commercial series of SPAN®, a_m varies from 40 Å^2 for SPAN® 20 (C12) to 37 Å^2 for SPAN® 40 (C16)[61] and from 40 Å^2 for MEGA-12 to 35 Å^2 for MEGA-14.

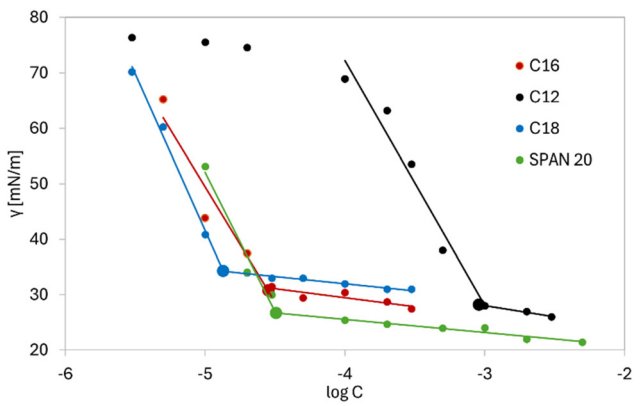

Fig. 7 GISA–amide surface tension reduction with concentration (log C). Evaluation of CMCs by intersection of the linear trends in pre- and post-micellar regimes.

Fig. 8 shows the results of the contact angle (CA) experiments. From these pictures, the CMC is visible again, but what is interesting in these graphs is the wetting behaviour in relation to the material of the surface. The polystyrene surface has a free energy from 35 to 44 mN m^{-1}, which indicates a relatively high energy surface, meaning it is weakly hydrophilic. When the water–surfactant solution is deposited on the PS, a lower surface tension (in terms of contact angle) is reached with 12-GISA-Amide, while higher surface tensions are reported for the 16- and 18-GISA-Amides, due to the fact that the surfactant with the shorter chain has more affinity for the quasi-hydrophilic surface. This does not happen with the PP surface, which has a surface free energy below 30 mN m^{-1}, which makes it quite a hydrophobic substrate.

The comparison of the behaviours of the surfactants on different materials highlights the necessity of combining different surfactants to obtain an optimal formulation. In detergents and coatings, for instance, maintaining a balance between long-chain and short-chain surfactants is crucial, as dirt particles can be either water-based or oil-based. Similarly, surfaces and textiles often consist of a diverse range of materials with different water/oil affinities.

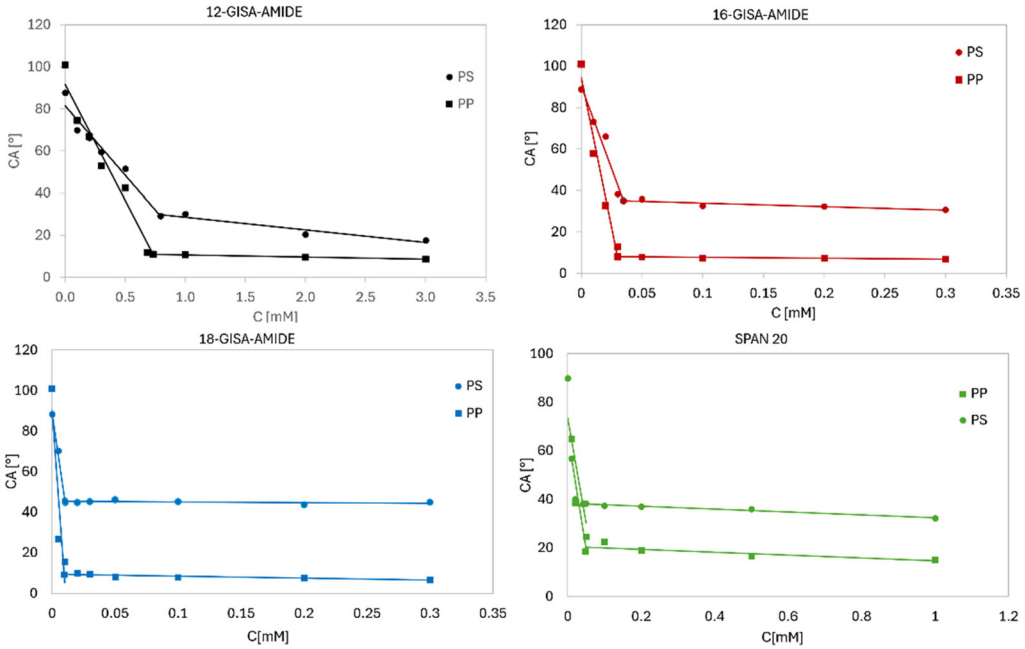

Fig. 8 Contact angle experiments for the three GISA–amide surfactants on PP and PS surfaces. Evaluation of CMC.

Table 10 HBL calculations using the different methods

Compound	HLB Davies	HLB Griffin	HLB Chemaxon
12-Amine	10.70	3.24	7.72
16-Amine	8.80	2.49	6.28
18-Amine	7.85	2.23	5.60
12-GISA-Amide	15.93	10.26	13.66
16-GISA-Amide	14.03	8.83	11.95
18-GISA-Amide	13.08	8.26	11.15
12-Lactamide	11.65	6.77	9.70
16-Lactamide	9.75	5.56	8.07
18-Lactamide	8.80	5.10	7.32
Sorbitan monolaurate	8.60	9.47	4.13
MEGA-12	17.35	11.78	15.12
MEGA-14	10.96	16.40	14.22

3.5 Hydrophilicity parameters

Hydrophilic–lipophilic balance (HLB). The HLB is a measure of the degree of hydrophilicity of amphiphilic molecules; it is mainly used in the field of formulation technology as an estimate of which kind of surfactant to use. The values obtained here are reported in Table 10, and they display substantial variations due to the differences explained in section 2.6.

Using the values proposed by the Griffin method enables the screening of possible applications and solubilities of surfactants based on their HLB. This HLB classification is broadly available in the literature (*e.g.*, ref. 66 and 67) and is not reported here. Considering the values of the HLB obtained for the GISA–amides, these molecules can be good stabilisers for O/W emulsions. However, the value of 18-GISA-Amide in particular is close to those of W/O stabilisers, so, in this case, the emulsion type is decided by other factors, such as phase ratio. The HLBs for the other compounds were calculated as well, since surfactants are usually never used alone but rather in mixtures. In fact, when making an emulsion, each oil has a required HBL for the O/W type and a required HBL for the W/O type; by matching these values, it is possible to forecast the type of emulsion that will be obtained. For example, to create an emulsion of stearic acid ($C_{18}H_{35}O_2$) requires a HBL of 15 for an O/W emulsion and a HBL of 6 for a W/O emulsion.[68] By mixing different surfactant molecules, the value of the HBL can be tuned to stabilise the emulsion using the lowest possible amount of surfactant, optimising the formulation in economic terms but also in terms of environmental impact and biocompatibility.

Partition coefficient. The partition coefficient can also be interpreted as a measure of the water and oil affinities of molecules. A good surface-active compound should have a $\log K_{OW}$ similar to the continuous phase but not drastically distant from the dispersed one. However, $\log K_{OW}$ is much more than a solubility parameter; indeed, it is used in the QSARs (quantitative structure–activity relationship). The QSARs are a series of mathematical models relating some quantitative parameters (*e.g.*, K_{OW} and molecular weight) derived from the chemical structure to a measure of a property or activity.[69] In surfactants, this can be used as a parameter to evaluate both the effect of surfactants on biological systems and the environmental impact, such as its toxicity as well as the possibility of applying it in drug delivery.

The $\log K_{OW}$ of some of the compounds involved in this research are reported in Table 11. Considering the average values of the available data, all the produced compounds,

Table 11 Estimated values, literature values and experimental values of the partition coefficients for the main synthetized surfactants

	Estimated				Experimental	
Compound	log K_{OW} Consensus	log K_{OW} Chemaxon	log K_{OW} ACDLabs	Average log K_{OW}	Literature	Exp.
12-Amine	4.30	3.7	4.90	4.3	4.76 [71]	—
16-Amine	6.03	5.35	7.12	6.2	6.73 [72]	—
18-Amine	6.92	6.14	8.19	7.1	7.7 [73]	—
12-GISA-Amide	1.59	0.68	2.42	1.6	—	0.82
16-GISA-Amide	3.37	2.27	4.54	3.4	—	2.3
18-GISA-Amide	4.26	3.06	5.61	4.3	—	2.9
12-Lactamide	3.83	3.27	4.38	3.8	3.79 [74]	—
16-Lactamide	5.60	4.86	6.50	5.7	5.35 [75]	—
18-Lactamide	6.49	5.65	8.56	6.9	7.78 [76]	—
Sorbitan monolaurate	2.57	1.77	4.47	2.93	3.15 [77]	—
MEGA-12	0.91	0.22	1.85	0.99	2.30[a] [78]	—
MEGA-14	1.80	1.01	2.91	1.90		—

[a] Value reported for a mix of 65–70% MEGA-12, 20–30% MEGA-14 and 0–15% C8 and C16.

except 16-lactamide and 18-lactamide, are in the range of intermediate values (1–4) of log K_{OW}, which is associated with moderate bioavailability, lower bioaccumulation, reasonable degradability, and less likelihood of exhibiting extreme mobility or persistence.[70]

Low partition coefficients (log K_{OW} < 0) means very hydrophilic compounds, which translate into greater bioavailability in water environments and hence easier hydrolysis and microbial degradation; however, they also spread widely and accumulate in aquatic organisms. On the other hand, high partition coefficients (log K_{OW} > 5) can be an index of accumulation in fatty tissues of organisms and persistence in environments, as they tend to adsorb in soils and sediments, making them less mobile and less available to bacterial degradation.[79] In general, extremely low or extremely high log K_{OW} values are associated with undesirable properties. The value of log K_{OW} is also used, together with others, as parameter to determine if a compound has the chemical and physical properties that are required for a drug-like molecule.[80]

According to the Ghose filter[81] and Lipinski's rule of five,[82] more than 80% of the drugs in the Comprehensive Medicinal Chemistry database have a log K_{OW} between −0.4 and 5.6 and a molecular weight between 180 and 500 Da. Values within this rage seem to indicate that the synthesized surfactant molecules have good biocompatibility: they have the right size and affinity to biological systems and for tissue permeation to be applied in pharmaceutical and cosmetic formulations. It is also possible that these compounds display antimicrobial activity. Clearly, these data alone are not enough to assess with certainty any of these properties, but, considering previous studies on the raw materials and on similar biobased surfactants, it is reasonable to think that these surfactants should not be harmful below a certain concentration and should have good biodegradability.

3.6 Solubility behaviour with temperature

When a solution is heated, the phase behaviour of surfactants can change, because their physical chemical characteristics are influenced by the energy of the molecules. With only a thermometer, it was possible to observe some interesting phenomena. When a 1% w/w solution was prepared, it was cloudy, while, when heated up instead at a certain temperature, it became clear. This temperature was different for the three chain lengths of the GISA surfactants: 23 °C, 39 °C, and 50 °C for the 12-, 16- and 18-GISA-Amides, respectively. The 16- and 18-GISA-Amides were not very soluble in water at room temperature. Cooling the solvent again resulted in reduced solubility of the surfactants and, consequently, a lower affinity between the solvent and the surfactant molecules. At this point, the molecules self-assembled into aggregates, present in high number since the concentration was greatly above the CMC, which interacted with one another and formed a three-dimensional network that immobilised the water molecules, causing gel-like behaviour.

3.7 Foam stability

Fig. 9 reports the foam height vs time for the three surfactants over a liquid height of 2 cm of a solution containing 1% w/w of surfactant in water. In agreement with the literature, which reports as foaming agents surfactants with alkyl chains of

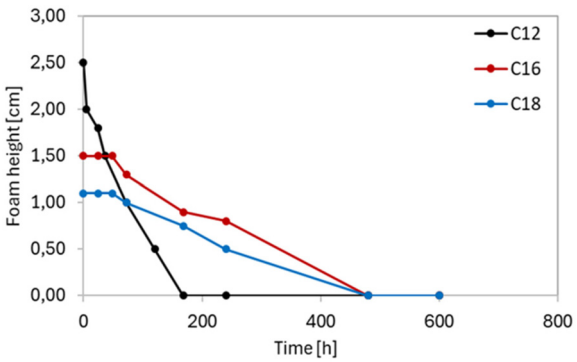

Fig. 9 Stability of the foam formed by GISA–amide surfactants in the cylinder shaking experiment.

10–14 carbons and HBLs of 10–15,[83,84–86] here as well the highest foam was obtained for 12-GISA-Amide. However, while this foam completely collapsed in a few days, for the longer chains, the small quantity of the formed foam was more durable, in accordance with reported trends. Sorbitan laurate, as expected, displayed very poor foaming capabilities due to its low HLB; this was expected, as this surfactant is usually applied as defoamer.[87] However, surfactants are practically never used singularly but in mixtures to obtain the best performance to quantity ratio. In particular, for foams, more often blends of non-ionic and ionic surfactants are used. From this foaming behaviour, however, some important statements can be made. 12-GISA-Amide has good foaming properties and could be suitable for those applications where foam is a desired or required property for consumers, such as shampoos. On the other hand, 16- and 18-GISA-Amides have lower but more persistent foaming, making them more suitable for home and industrial cleaning.

3.8 Emulsions stability

Upon shaking the octanol–water system used for log K_{OW} (1 : 1 octanol:1% surfactant solution), the system stabilized in a Winsor type III system, composed of three layers: the water phase, the O/W emulsion and the oil on the top layer. The system remained stable for more than one month. The O/W emulsions containing both 1% surfactants and 2% surfactants (refer to Table 2) also remained stable for more than one month. In contrast, 12-GISA-Amide was not able to stabilise the W/O emulsion, while 16- and 18-GISA-Amides did. These results were expected, as the required HLB for sunflower seed oil is 11 for an O/W emulsion, which is close enough to the HLBs of all three surfactants, while the required HLB for a W/O emulsion is 7, which is very different from the HLB of 12-GISA-Amide. Sorbitan laurate, due to its higher hydrophobicity compared to the GISA surfactants, was able to stabilise only the W/O emulsion in these conditions.

4. Conclusions

This work shows the possibility of valorising side streams, such as pulping liquors and other cellulose-containing waste, for the production of added-value surfactants, thus addressing two important environmental issues, specifically non-sustainable surfactant synthesis and their raw materials and the end of life of these molecules. Here, surfactants with excellent characteristics were produced by exploiting different cellulose sources, including waste materials such as sedimented pulp mill waste (ZFS) and lactose. These were treated with NaOH to obtain hydroxy acid mixtures and were used without any pre-purification. In addition, these molecules were produced in relatively short reaction times, at room temperature, with only the addition of water and mechanical stimuli. In the mortar, yields up to 95% were achieved from a purchased GISA (GISA_STN_16), up to 75% with MCC HAs (MCC_12_PM) and up to 70% with the ZFS HAs (ZFS_12_PM). In the ball mill, the maximum achieved yield was 85% (MCC_18_MILL15). The downstream purification was done by exploiting the foaming capability of the surfactant mixtures; foam fractionation only required the solubilisation of surfactants and the use of low-pressure air flow to achieve an increase in yield up to 33% for MCC_12_PM. Improving the foam fractionation design and operation could lead to higher purities. The GISA–Amide surfactants represented the main focus of the present work and showed CMCs of 0.76, 0.033 and 0.012, respectively, proportional to the alkyl chain length; foam height decreased with increasing chain length, while the stability had the opposite trend. Exploiting some computational tools together with experiments, it was possible to estimate the partition coefficients for the main compounds, which give credit to the hypothesis of the excellent biocompatibility of these surfactants, as previously suggested by studies on the raw materials and on similar compounds. Finally, the comparison with commercially available surfactants, especially MEGAs, also showed the great potential of the GISA–amides. In fact, the GISA–amides displayed highly comparable parameters to MEGAs due to their extreme similarity in chemical structure, confirming the initial hypothesis that GISA surfactants can be possible substitutes for sugar-based surfactants. When compared to sorbitan laurate, the GISA–amides showed higher hydrophilicity; in fact, some of the parameters of sorbitan laurate were more similar to those of 18-GISA-Amide than 12-GISA-Amide due to the chemical difference between the ester and the amide bond and the higher number of free –OH groups in GISA than in sorbitan.

Conflicts of interest

There are no conflicts to declare.

Data availability

The data supporting this article have been provided in the manuscript, and additional data have been included as part of the ESI.†

Acknowledgements

The authors thank Prof. Rama Layek for the NMR analysis, MSc. Lauri Saukkonen and Milla Mattila for their contributions in the study of the hydroxy acid mixtures. Open Access funding was provided by LUT University (previously Lappeenranta University of Technology (LUT)). Financial support from Business Finland (5R Refinery project, ID 43303/31/2020) is gratefully acknowledged as well as fundings from LUT doctoral school.

References

1 S. O. Badmus, H. K. Amusa, T. A. Oyehan and T. A. Saleh, *Environ. Sci. Pollut. Res.*, 2021, **28**, 62085–62104.
2 M. Palmer and H. Hatley, *Water Res.*, 2018, **147**, 60–72.

3 R. Alén, in *Industrial Biorefineries & White Biotechnology*, ed. A. Pandey, R. Höfer, M. Taherzadeh, K. M. Nampoothiri and C. Larroche, Elsevier, Amsterdam, 2015, pp. 91–126.
4 C. Knill and J. Kennedy, *Carbohydr. Polym.*, 2003, **51**, 281–300.
5 I. Pavasars, J. Hagberg, H. Borén and B. Allard, *J. Polym. Environ.*, 2003, **11**, 39–47.
6 J. Heinonen and T. Sainio, *Sep. Purif. Technol.*, 2019, **221**, 349–362.
7 L. Reyes, C. Nikitine, L. Vilcocq and P. Fongarland, *Green Chem.*, 2020, **22**, 8097–8115.
8 M. Lewin and L. G. Roldan, *Text. Res. J.*, 1975, **45**, 308–314.
9 H. B. Klinke, B. K. Ahring, A. S. Schmidt and A. B. Thomsen, *Bioresour. Technol.*, 2002, **82**, 15–26.
10 M. Mattila, L. Saukkonen, J. Laine, J. Heinonen and T. Sainio, *Waste Biomass Valorization*, 2025, DOI: **10.1007/s12649-025-02990-1**.
11 M. A. Glaus and L. R. Van Loon, *Environ. Sci. Technol.*, 2008, **42**, 2906–2911.
12 J. Tits, E. Wieland and M. H. Bradbury, *Appl. Geochem.*, 2005, **20**(11), 2082–2096.
13 P. Warwick, N. Evans, T. Hall and S. Vines, *Radiochim. Acta*, 2004, **92**, 897–902.
14 P. Warwick, N. Evans and S. Vines, *Radiochim. Acta*, 2006, **94**, 363–368.
15 M. Almond, M. G. Suleiman, M. Hawkins, D. Winder, T. Robshaw, M. Waddoups, P. N. Humphreys and A. P. Laws, *Carbohydr. Res.*, 2018, **455**, 97–105.
16 D. K. Allen and B. Y. Tao, *J. Surfactants Deterg.*, 1999, **2**, 383–390.
17 D. Tripathy, D. Gupta, A. Jain and A. Mishra, *Surfactants from Renewable Raw Materials*, 2021.
18 A. Tehrani-Bagha and K. Holmberg, *Curr. Opin. Colloid Interface Sci.*, 2007, **12**, 81–91.
19 I. J. A. Baker, R. I. Willing, D. N. Furlong, F. Grieser and C. J. Drummond, *J. Surfactants Deterg.*, 2000, **3**, 13–27.
20 H. Oskarsson, M. Frankenberg, A. Annerling and K. Holmberg, *J. Surfactants Deterg.*, 2007, **10**, 41–52.
21 H. Kumar and R. Alén, *Sustainable Chem. Processes*, 2016, **4**(4).
22 M. Reintjes and G. K. Cooper, *Ind. Eng. Chem. Prod. Res. Dev.*, 1984, **23**, 70–73.
23 G. Li, S. Ma and M. Szostak, *Trends Chem.*, 2020, **2**, 914–928.
24 R. Bordes, J. Tropsch and K. Holmberg, *Langmuir*, 2010, **26**, 3077–3083.
25 T. H. Ali, R. S. D. Hussen and T. Heidelberg, *Colloids Surf., B*, 2014, **123**, 981–985.
26 A. Hinzmann and H. Gröger, *Eur. J. Lipid Sci. Technol.*, 2020, **122**, 1900163.
27 J. Barrault, M. Seffen, C. Forquy and R. Brouard, in *Studies in Surface Science and Catalysis*, ed. M. Guisnet, J. Barrault, C. Bouchoule, D. Duprez, C. Montassier and G. Pérot, Elsevier, 1988, vol. 41, pp. 361–369.
28 S. Nuraliev, U. Berdiyarov, S. Nurmanov and O. Kodirov, *Univ. Tehn. Nauki*, 2024, **5**, 62–70.
29 R. Coeck and D. E. D. Vos, *Green Chem.*, 2020, **22**, 5105–5114.
30 J. Citoler, S. R. Derrington, J. L. Galman, H. Bevinakatti and N. J. Turner, *Green Chem.*, 2019, **21**, 4932–4935.
31 J. Citoler, W. Finnigan, H. Bevinakatti and N. J. Turner, *ChemBioChem*, 2022, **23**, e202100578.
32 J. Magano, *Org. Process Res. Dev.*, 2022, **26**, 1562–1689.
33 T. Nikonovich, T. Jarg, J. Martõnova, A. Kudrjašov, D. Merzhyievskyi, M. Kudrjašova, F. Gallou, R. Aav and D. Kananovich, *RSC Mechanochem.*, 2024, **1**, 189–195.
34 T. Nikonovich, Doctoral Diseration, Tallinn Unversity of Technology, 2024.
35 D. Tan, L. Loots and T. Friščić, *Chem. Commun.*, 2016, **52**, 7760–7781.
36 P. Ying, J. Yu and W. Su, *Adv. Synth. Catal.*, 2021, **363**, 1246–1271.
37 A. Bil, B. Abdellahi, G. Pourceau and A. Wadouachi, *Sustainable Chem.*, 2022, **3**, 300–311.
38 F. Bensebaa, in *Interface Science and Technology*, ed. F. Bensebaa, Elsevier, 2013, vol. 19, pp. 147–184.
39 C. Herrlé, S. Toumieux, M. Araujo, A. Peru, F. Allais and A. Wadouachi, *Green Chem.*, 2022, **24**, 5856–5861.
40 N. Tharapiwattananon, J. F. Scamehorn, S. Osuwan, J. H. Harwell and K. J. Haller, *Sep. Sci. Technol.*, 1996, **31**, 1233–1258.
41 S. S. Srinet, A. Basak, P. Ghosh and J. Chatterjee, *J. Environ. Chem. Eng.*, 2017, **5**, 1586–1598.
42 R. Lemlich, *Ind. Eng. Chem.*, 1968, **60**, 16–29.
43 C.-Y. Chen, S. C. Baker and R. C. Darton, *J. Chem. Technol. Biotechnol.*, 2006, **81**, 1915–1922.
44 C.-Y. Chen, S. C. Baker and R. C. Darton, *J. Chem. Technol. Biotechnol.*, 2006, **81**, 1923–1931.
45 R. Li, Z. L. Wu, Y. J. Wang and L. L. Li, *Ind. Crops Prod.*, 2013, **51**, 163–170.
46 T.-H. Zhao, J.-Y. Gu, W.-F. Pu, Z.-M. Dong and R. Liu, *RSC Adv.*, 2016, **6**, 70165–70173.
47 K. A. Wilk, L. Syper, B. Burczyk, A. Sokołowski and B. W. Domagalska, *J. Surfactants Deterg.*, 2000, **3**, 185–192.
48 O. M. Haghighi, G. Zargar, A. Khaksar Manshad, M. Ali, M. A. Takassi, J. A. Ali and A. Keshavarz, *Energies*, 2020, **13**, 3988.
49 T. Kato, T. Nakamura, M. Yamashita, M. Kawaguchi, T. Kato and T. Itoh, *J. Surfactants Deterg.*, 2003, **6**, 331–337.
50 C. Boyat, V. Rolland-Fulcrand, M.-L. Roumestant, Ph. Viallefont and J. Martinez, *Prep. Biochem. Biotechnol.*, 2000, **30**, 281–294.
51 P. Hennaux and A. Laschewsky, *Colloid Polym. Sci.*, 2003, **281**, 807–814.
52 W. C. Griffin, *J. Soc. Cosmet. Chem.*, 1954, **5**, 249–256.
53 J. T. Davies, *Proc. Int. Congr. Surf. Act.*, 1957, 426–438.
54 R. Barret, in *Therapeutical Chemistry*, ed. R. Barret, Elsevier, 2018, pp. 53–78.
55 *Marvin – Chemical Drawing Software*, **https://chemaxon.com/marvin**, (accessed January 20, 2025).

56 V. N. Viswanadhan, A. K. Ghose, G. R. Revankar and R. K. Robins, *Math. Comput. Modell.*, 1990, **14**, 505–510.
57 G. Klopman, J.-Y. Li, S. Wang and M. Dimayuga, *J. Chem. Inf. Comput. Sci.*, 1994, **34**, 752–781.
58 R. Campana, A. Merli, M. Verboni, F. Biondo, G. Favi, A. Duranti and S. Lucarini, *Pharmaceuticals*, 2019, **12**, 186.
59 K. Niemelä, *Biomass*, 1988, **15**, 223–231.
60 J. Käkölä, R. Alén, H. Pakkanen, R. Matilainen and K. Lahti, *J. Chromatogr., A*, 2007, **1139**, 263–270.
61 L. J. Peltonen and J. Yliruusi, *J. Colloid Interface Sci.*, 2000, **227**, 1–6.
62 M. R. Porter, in *Handbook of Surfactants*, ed. M. R. Porter, Springer US, Boston, MA, 1991, pp. 49–53.
63 Y.-P. Zhu, M. J. Rosen, P. K. Vinson and S. W. Morrall, *J. Surfactants Deterg.*, 1999, **2**, 357–362.
64 A. Walter, S. E. Suchy and P. K. Vinson, *Biochim. Biophys. Acta*, 1990, **1029**, 67–74.
65 M. J. Rosen and J. T. Kunjappu, Adsorption of Surface-Active Agents at Interfaces: The Electrical Double Layer. *In Surfactants and Interfacial Phenomena*, 2012.
66 Q. Chang, in *Colloid and Interface Chemistry for Water Quality Control*, ed. Q. Chang, Academic Press, 2016, pp. 227–245.
67 W. C. Griffin, *J. Soc. Cosmet. Chem.*, 1949, **1**, 311–326.
68 Reference Guide to HLB Values of Common Emulsifiers – Alfa Chemistry, **https://cosmetics.alfa-chemistry.com/resources/reference-guide-to-hlb-values-of-common-emulsifiers.html**, (accessed January 21, 2025).
69 QSAR models – ECHA, **https://echa.europa.eu/support/registration/how-to-avoid-unnecessary-testing-on-animals/qsar-models**, (accessed January 20, 2025).
70 C. Isarankura-Na-Ayudhya, T. Naenna, C. Nantasenamat and V. Prachayasittikul, *Excli J.*, 2009, **8**, 74–88.
71 ICSC 1364 – DODECYLAMINE, **https://webapps.ilo.org/dyn/icsc/showcard.display?p_lang=en&p_card_id=1364&p_version=2**, (accessed January 21, 2025).
72 Sigma Aldrich, Safety Datasheet Hexadecylamine, **https://www.sigmaaldrich.com/FI/en/sds/aldrich/445312?userType=anonymous**, (accessed January 21, 2025).
73 ICSC 1365 – OCTADECYLAMINE, **https://www.inchem.org/documents/icsc/icsc/eics1365.htm**, (accessed January 21, 2025).
74 N-dodecyl-2-hydroxy-propanamide, **https://www.chemsrc.com/en/cas/5422-41-3_958162.html**, (accessed January 21, 2025).
75 N-HEXADECYL-2-HYDROXYPROPANAMIDE |5323-53-5-Molbase, **https://www.molbase.com/moldata/1500848.html**, (accessed January 21, 2025).
76 2-HYDROXY-N-OCTADECYL-PROPANAMIDE – Chemical Details, **https://comptox.epa.gov/dashboard/chemical/details/DTXSID00279032**, (accessed January 21, 2025).
77 V. Bampidis, G. Azimonti, M. d. L. Bastos, H. Christensen, B. Dusemund, M. Kouba, M. Kos Durjava, M. López-Alonso, S. López Puente, F. Marcon, B. Mayo, A. Pechová, M. Petkova, F. Ramos, Y. Sanz, R. E. Villa, R. Woutersen, G. Aquilina, G. Bories, A. Chesson, C. Nebbia, D. Renshaw, M. L. Innocenti and J. Gropp, *EFSA J.*, 2019, **17**, e05651.
78 Australian Government, Department of Health. National Industrial Chemicals. Existing Chemical Secondary Notification Assessment Report STD/735S. D-glucitol, 1-deoxy-1-(methylamino)-, N-C10-16 acyl derivatives. June 2017.
79 J. C. Dearden, *Environ. Health Perspect.*, 1985, **61**, 203–228.
80 C. I. Cappelli, E. Benfenati and J. Cester, *Environ. Res.*, 2015, **143**, 26–32.
81 S. Kralj, M. Jukič and U. Bren, *Encyclopedia*, 2023, **3**, 501–511.
82 C. A. Lipinski, F. Lombardo, B. W. Dominy and P. J. Feeney, *Adv. Drug Delivery Rev.*, 1997, **23**, 3–25.
83 S. Mistry, HLB Scale (Hydrophilic Lipophilic Balance), **https://solutionpharmacy.in/hlb-scale/**, (accessed June 20, 2023).
84 Y. Zhou, S. Wang, M. Lv, J. Niu and B. Xu, *J. Surfactants Deterg.*, 2017, **20**, 623–630.
85 M. J. Rosen and J. T. Kunjappu, in *Surfactants and Interfacial Phenomena*, 2012, pp. 308–335.
86 D. Myers, in *Surfactant Science and Technology*, 2005, pp. 245–279.
87 J. R. Brunner, *J. Dairy Sci.*, 1950, **33**, 741–746.